

## First results of IBIS/ISGRI Cygnus X-3 monitoring during INTEGRAL PV phase<sup>★</sup>

P. Goldoni, J. M. Bonnet-Bidaud, M. Falanga, and A. Goldwurm

CEA Saclay, DSM/DAPNIA/Service d'Astrophysique, 91191 Gif-sur-Yvette, France

Received 14 July 2003 / Accepted 10 September 2003

**Abstract.** We report on preliminary results of IBIS/ISGRI serendipitous observations of Cygnus X-3 in the 15–100 keV energy range during the INTEGRAL Performance and Verification phase. This peculiar microquasar was inside IBIS/ISGRI field of view at a  $\sim 9^\circ$  distance from the pointing direction during Cygnus X-1 staring observations in November and December 2002. We analyzed observations from 27 November 2002 to 8 December 2002 with an effective on source exposure time of  $\sim 300$  ks. Cyg X-3 was always significantly detected in the 15–40 and 40–100 keV energy bands during single exposures lasting between 30 min and one hour. The source light curve shows the characteristic 4.8-hour modulation with a shape consistent with a standard template. The two light curves' phase zero have no measurable offset and their values are consistent with historical ephemeris. These results show that even at this early stage of the mission, IBIS/ISGRI is capable of producing high quality scientific results on highly off axis, relatively bright targets.

**Key words.** X-ray binaries – coded mask instruments

### 1. Introduction

Cygnus X-3 is an enigmatic X-ray binary which does not fit well into any of the established classes of X-ray binaries (see Bonnet-Bidaud & Chardin 1988 for a review). One of its main characteristics is a 4.8-hour modulation visible in hard X-rays (Hermsen et al. 1987; Robinson et al. 1997), soft X-rays (Parsignault et al. 1972) and infrared (Becklin et al. 1972; Mason et al. 1986). If interpreted as the orbital period, this modulation would imply that Cyg X-3 is a low mass X-ray binary, but infrared observations suggest that the donor star is a Wolf-Rayet star (van Kerkwijk et al. 1992). Due to its heavy absorption, no optical counterpart has been found. The true nature of the compact object has not been revealed despite orbital-phase-resolved spectroscopy performed in infrared (Hanson et al. 2000).

Cyg X-3 is also a strong source of radio emission with different behaviors: 1) quiescence (60–100 mJy), 2) major flaring (greater than 1 Jy) with quenching (very low fluxes  $\sim 10$ –20 mJy) 3) minor flaring (less than 1 Jy) with partial quenching. During major radio outbursts jet-like structures have been detected moving at a velocity of either 0.8 or 0.5 c depending on whether the jets are one-sided or double-sided

(Mioduszewski et al. 2001; Martí et al. 2002). This is particularly interesting in the context of models where hard X-ray emission is originated in a low-level jet (see e.g. Markoff et al. 2003).

Soft X-ray emission has been observed to undergo high and low states in which the various spectral components change with no apparent correlation with other properties (White et al. 1995). Hard X-ray emission has been extensively monitored with BATSE in the 20–100 keV band with the Earth occultation method. The results have been reported by McCollough et al. (1999) for the period 1991–1996. This monitoring allowed the construction of light curves with a 3-day time-scale. The two most distinctive features of these light curves are extended periods of high flux (150–300 mCrab) and low flux periods when the source was undetectable. The 20–100 keV flux is correlated with radio emission during flaring activity and anti-correlated during the quenched radio state. The relationship between hard X-rays and radio emission may be an indication of the non thermal nature of the hard X-ray emission. However, BATSE results were simply fitted with a power law with photon index  $\alpha = 3$  with no further spectral analysis.

A unified spectral X-ray model based on GINGA data (2–37 keV) was proposed by Nakamura et al. (1993). It includes several different components including a blackbody, a power law with cutoff, an iron line and dust absorption. This model properly fits soft X-ray data, but it cannot be used to address the issue of the origin of X-ray emission over 40 keV. Indeed, BeppoSAX observations in 1999 indicate deviations from this behavior (Palazzi et al. 1999) at hard X-ray energies.

Send offprint requests to: P. Goldoni,  
e-mail: pgoldoni@cea.fr

<sup>★</sup> Based on observations with INTEGRAL, an ESA project with instruments and science data center funded by ESA member states (especially the PI countries: Denmark, France, Germany, Italy, Switzerland, Spain), Czech Republic and Poland, and with the participation of Russia and the USA.

We report here on the first results of INTEGRAL/ISGRI observation of Cyg X-3 during the Performance and Verification phase. The source was serendipitously observed for more than one month during PV phase observations dedicated to Cyg X-1. The combination of high energy sensitivity and exposure of these observations is unprecedented for Cyg X-3.

## 2. Observations

The INTEGRAL satellite (Winkler et al. 2003) is an ESA observatory dedicated to 15 keV–10 MeV  $\gamma$ -ray observations with concurrent source monitoring in X-rays (3–35 keV) and in the optical range ( $V$ , 500–600 nm). The INTEGRAL payload consists of two main  $\gamma$ -ray instruments, the spectrometer SPI (Vedrenne et al. 2003) and the imager IBIS, and of two monitor instruments, the X-ray monitor JEM-X (Lund et al. 2003) and the Optical Monitoring Camera OMC (Mas-Hesse et al. 2003).

The imaging performances of IBIS (Ubertini et al. 2003) are characterized by the coupling of its source discrimination capability with a very wide field of view (FOV), namely  $9^\circ \times 9^\circ$  fully coded,  $29^\circ \times 29^\circ$  partially coded FOV. It consists of two detection layers, ISGRI and PICsIT, optimized for lower and higher energy sensitivity. The upper one, ISGRI (Lebrun et al. 2003) is sensitive between 15 keV and 1 MeV while its peak sensitivity is between 15 keV and 200 keV. The lower one, PICsIT (Di Cocco et al. 2003) is sensitive between  $\sim 200$  keV and  $\sim 8$  MeV.

During its Performance and Verification Phase INTEGRAL observed the Cygnus region from 15 November 2002 to 23 December 2002. The main target of the PV phase was the Black Hole candidate Cygnus X-1 which was observed on axis and at different off axis distances (Bazzano et al. 2003; Laurent et al. 2003). During the main part of these observations Cyg X-3 was contained in the field of view of the main instruments IBIS and SPI. We report here on results of observations of the ISGRI camera of the IBIS telescope.

During the first weeks of observations, the instrument parameters were frequently modified to optimize the instrument performances. Moreover, the pointing direction frequently changed. For our analysis, we limit ourselves to observations performed in the period between 27 November 2002 and 8 December 2002 when the satellite was performing staring observations on Cyg X-1. Results of later observations on December 22–23 are described in Vilhu et al. (2003).

During the selected period the total observing time is  $\sim 5.6 \times 10^5$  s but due to the off axis position, the effective exposure time on Cyg X-3 is  $\sim 3.2 \times 10^5$  s. These observations were performed during 4 orbits (revolutions) and they were split into separate “science windows” lasting 1800 to 3600 s (see Table 1 for details). The distance of Cyg X-3 from the pointing direction was about  $8.8^\circ$ . This distance corresponds to a coded area or relative sensitivity of 57% for ISGRI.

The images produced by the telescope were analyzed using the ISDC public software and software developed at our institute for calibration purposes. The images were deconvolved using the procedures described in Goldwurm et al. (2003) to recover source position and flux.

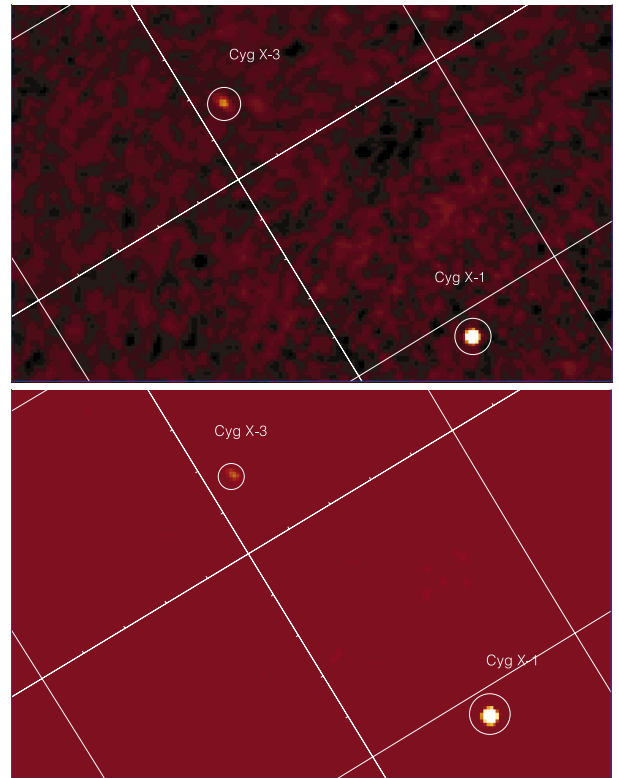


**Fig. 1.** 15–40 keV (top) and 40–100 keV deconvolution images of IBIS/ISGRI observations during revolution 16. They result from the sum of 56 Science Window of duration varying between 1800 and 3600 s for a total of  $\sim 147$  ks. The confidence levels start from  $10\sigma$  and are linearly spaced. The white grid represents Galactic Coordinates, the lines are spaced by 6 degrees. Cyg X-1 is at the bottom left and is detected at  $\sim 1000\sigma$  and  $\sim 850\sigma$  level respectively, Cyg X-3 is on top right at  $\sim 160\sigma$  and  $\sim 55\sigma$  level respectively

## 3. Imaging analysis and light curves

For every science window we produced deconvolved images in three energy bands: 15–40 keV, 40–100 keV and 100–200 keV. The images of the same revolution were then summed to attain higher sensitivity (see Fig. 1). In the two lower energy bands Cyg X-3 is detected at a level of confidence between 10 and  $20\sigma$  in the majority of the science windows. The offset of the measured position with respect to the position in the catalog is between 0 and 4 arcmin (i.e. less than a pixel), which is compatible with expected results for an off axis source of this intensity. The main count rate in the 15–40 keV band varied between 35 cts/s and 10 cts/s, while the 40–100 keV count rate was between 15 cts/s and 2 cts/s. Correlated variations in the 2 energy bands on the time-scales of days are clearly visible. In the 100–200 keV energy band Cyg X-3 was not consistently detected in single exposure while it was detected in the summed images lasting 150 ks or more at a level of  $\sim 10\sigma$ . However the flux value is difficult to estimate as it is near the background level. We therefore limited our analysis to the first two energy bands. The flux ratio between the two lower energy bands indicate a very soft spectrum with photon index  $\alpha \sim 3$ .

We estimated Cyg X-3 flux using the ISGRI count rate of the Crab nebula at an off axis angle similar to the Cyg X-3 one

**Table 1.** Observation log and average fluxes of Cyg X-3 in the period 27/11/2002–08/12/2002. The pointing direction was constant at 19h 58m 21.7s +35° 12' 05", Cyg X-3 was 8.8° off axis with a coded fraction of 57%. The 4 periods correspond to revolution 15 to 18 and are divided into single observations of duration varying between 1800 and 3600 s. Between each period there is a perigee passage lasting about half a day. The shorter exposure time in revolution 17 is due to the absence of reliable data during a long period (see also Fig. 2). We estimated the average fluxes in milliCrab using Crab nebula observations at a similar off axis angle and added a 5% systematic error.

Obs. start–stop (JD–2 440 000)	Duration (s)	Eff. exp. (s)	15–40 keV Flux (mCrab)	40–100 keV Flux (mCrab)
52 605.9–52 608.5	153 340	87 400	125 ± 6	60 ± 3
52 608.9–52 611.5	146 810	83 680	137 ± 3.5	58 ± 3
52 611.9–52 612.3	81 230	46 300	150 ± 7.5	70 ± 3.5
52 614.9–52 617.5	179 040	102 050	137 ± 3.5	59 ± 3

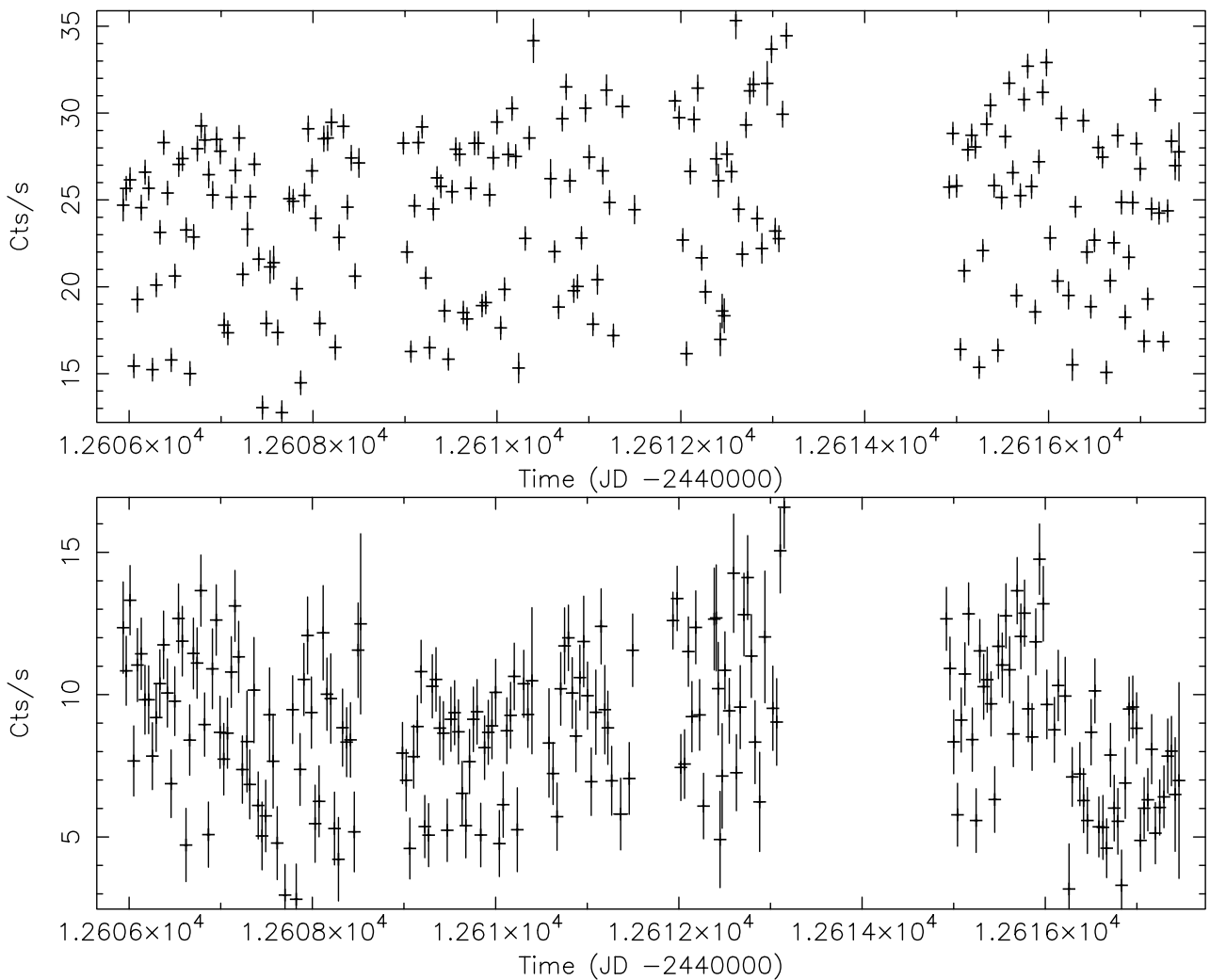


**Fig. 2.** Cyg X-3 15–40 keV (*top panel*) and 40–100 keV (*bottom panel*) light curves for revolutions 15 to 18. The horizontal time scale is in days. Each point represents a science window of duration varying between 1800 and 3600 s. Periodic gaps in the data are due to radiation belt passes while the longer gap at day  $1.2614 \times 10^4$  is due to a data loss. The point to point variation reflect the 4.8-hour modulation.

in our observations. From these first results it is apparent that the source was in the high hard X-ray flux state seen by BATSE, its flux being stronger than 100 mCrab in the low energy band.

### 3.1. Period folding

The evolution of the average source flux is shown in Fig. 2. Variations around the average value on the time-scale of less

than a day are clearly visible in the light curve at both energies. The point-to-point variations reflect the effect of the 4.8-hour modulation. We folded both source light curves with a 4.8-hour period (Fig. 3). The shape of the folded light curves are found to be very similar to the long term average shape of the light curve obtained at lower energy and are fitted nicely with the normalized X-ray template of van der Klis & Bonnet-Bidaud (Bonnet Bidaud & Chardin 1988). Small variations are

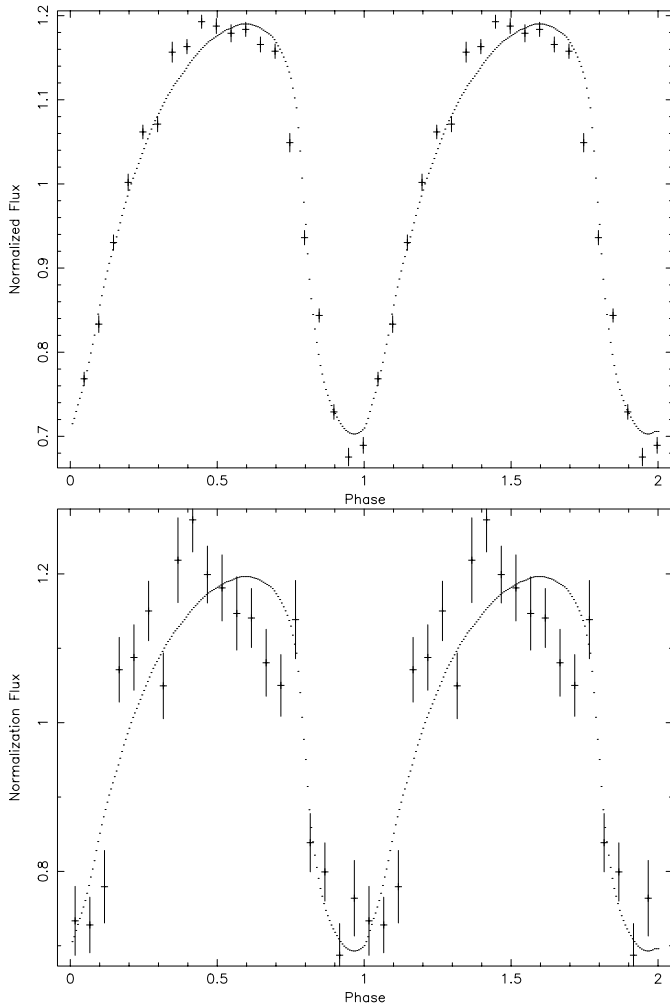


**Fig. 3.** Cyg X-3 light curves in the 15–40 keV (*top panel*) and 40–100 keV (*bottom panel*) energy bands folded to the 4.8-hour period using the template from van der Klis & Bonnet-Bidaud (1989).

however visible in the rising part of the curve. Therefore the arrival time of the minimum of the folded light curve was derived by cross-correlating the folded data with the standard template in the restricted phase range of [0.75–1.25]. To take into account systematic uncertainties, the statistical errors were scaled by a constant factor to make them fit the template with a reduced  $\chi^2$  of 1.0. This analysis yielded a heliocentric minimum arrival time of (HJD 2 452 606.06446 $\pm$ 0.0017) in the 15–40 keV range. Fitting with the overall light curve does not introduce a significant shift. The new INTEGRAL arrival point is plotted in Fig. 4 alongside with previous results (see Singh et al. 2002) and fits nicely with published ephemeris of Cyg X-3 thus validating our analysis. A new ephemeris was computed by fitting a cubic function indicated by previous studies (van der Klis & Bonnet-Bidaud 1989; Singh et al. 2002). The INTEGRAL observations confirm the existence of a significant rate of change of the period derivative. We obtain a significant nonzero value of  $\dot{P} = -(2.2 \pm 1.5) \times 10^{-11} \text{ yr}^{-1}$ , strengthening the last published value of  $\dot{P} = -(1.3 \pm 1.6) \times 10^{-11} \text{ yr}^{-1}$  (Singh et al. 2002). Future INTEGRAL monitoring during the core program will allow to gain better precision on this term.

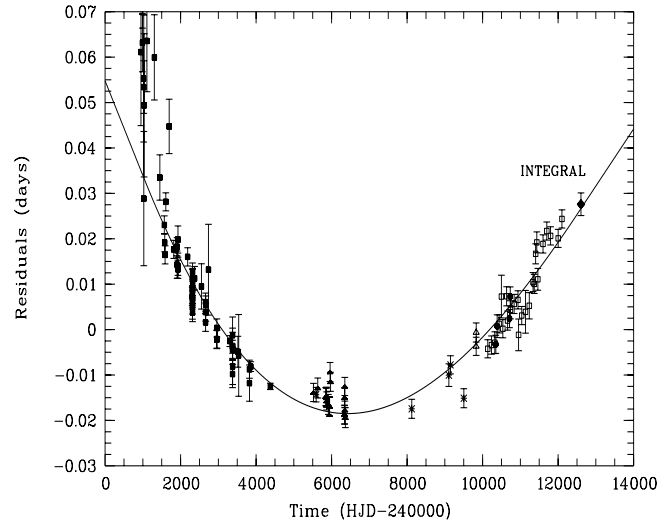


**Fig. 4.** Cyg X-3 arrival times residuals with respect to the linear ephemeris of Singh et al. (2002). Different symbols are for data earlier than 1983 (filled squares), EXOSAT (filled triangles), Tenma, GINGA and ASCA (asterisks), ROSAT (open triangles), XTE/ASM (open squares), BeppoSAX (filled circles) and INTEGRAL (filled lozenge). Also shown is the best fitted cubic ephemeris with a significant slowing down of the period derivative.

We checked for the possible presence of a time delay between the hard (40–100 keV) and the soft energy (15–40 keV) light curves. Indeed, Matz (1997) reported a 6–7  $\sigma$  evidence of a constant time delay of  $\sim 20$  min between XTE/ASM (2–12 keV) and OSSE (44–130 keV) data. We correlated the two light curves with the template in the restricted phase range of [0.75–1.25] and measured the difference in the minimum arrival times obtained. We found no measurable time delay between the two light curves. The (hard-soft) difference in the minimum arrival times is estimated to be  $\Delta t = -(5.5 \pm 8.6)$  minutes where the error bar is at a  $3\sigma$  level. We therefore do not confirm the presence of a time delay between soft and hard X-rays at this level.

#### 4. Conclusions

We report on first results of the ISGRI/IBIS detector on-board the INTEGRAL observatory for the peculiar microquasar Cyg X-3. The source was serendipitously observed during Cyg X-1 Performance and Verification Phase observations and during the observations we selected it was off axis by 8.8°.

We demonstrate that, despite the a priori unfavorable position of the source in the FOV, we are able to obtain high quality results. Even if at this stage of data analysis, the results are still preliminary, we demonstrate that the 4.8-hour modulation is clearly visible. Moreover the absolute time of the phase zero is fully consistent with previously published data. No measurable time delay could be found between the two light curves.

The light curve shape that we obtain for the two energy bands possibly indicates that the same physical mechanism is responsible for the bulk of photon emission between 15 and 100 keV.

Even at this early stage of the mission, we demonstrate the IBIS/ISGRI detector capability of producing scientific results for relatively bright ( $>50$  mCrab), off axis targets. This capability is one of the most important IBIS/ISGRI characteristics and its exploitation will be very important throughout the mission.

## References

- Bazzano, A., Bird, A. J., Capitanio, F., et al. 2003, *A&A*, 411, L389
- Becklin, E. E., Kristian, J., Neugebauer, G., et al. 1972, *Nature Phys. Sci.*, 239, 134
- Bonnet-Bidaud, J. M., & Chardin, G. 1988, *Phys. Rep.*, 170, 326
- Di Cocco, G., Caroli, E., Celesti, E., et al. 2003, *A&A*, 411, L189
- Goldwurm, A., David, P., Foschini, L., et al. 2003, *A&A*, 411, L223
- Hanson, M. M., Still, M. D., & Fender, R. P. 2000, *ApJ*, 541, 308
- Hermesen, W., Bloemen, J. B. G. M., Jansen, F. A., et al. 1987, *A&A*, 175, 141
- Laurent, P., Cadolle Bel, M., Bazzano, A., et al. 2003, *A&A*, submitted
- Lebrun, F., Leray J.-P., Lavocat, Ph., et al. 2003, *A&A*, 411, L141
- Lund, N., Brandt, S., Budtz-Joergensen, C., et al. 2003, *A&A*, 411, L231
- McCollough, M. L., Robinson, C. R., Zhang, S. N., et al. 1999, *A&A*, 86, 286
- Markoff, S., Nowak, M., Corbel, S., et al. 2003, *A&A*, 397, 645
- Martí, J., Paredes, J. M., & Peracaula, M. 2002, in *Proc. fourth MicroQuasars Workshop*, ed. Ph. Dourouchoux, Y. Fuchs, & J. Rodriguez, Center for Space Physics: Kolkata (India), 205
- Mas-Hesse, M., Gimenez, A., Culhane, L., et al. 2003, *A&A*, 411, L261
- Mason, K. O., Cordova, F. A., & White, N. E. 1986, *ApJ*, 309, 700
- Matz, S. M. 1997, *Proc. Fourth Compton Symposium*, ed. C. D. Dermer, M. S. Strickman, & J. D. Kurfess (Williamsburg), VA April 1997, *AIP Conf. Proc.*, 410, 808
- Mioduszewski, A. J., Rupen, M. P., Hjellming, R. M., et al. 2001, *ApJ*, 553, 766
- Nakamura, H., Matsuoka, M., Kawai, N., et al. 1993, *MNRAS*, 261, 353
- Palazzi, E., Nicastro, L., Orlandini, M., et al. 1999, *Ap. Lett. & Comm.*, 38, 109
- Parsignault, D. R., Gursky, H., Kellogg, E. M., et al. 1972, *Nature Phys. Sci.*, 239, 123
- Robinson, C. R., Harmon, B. A., McCollough, M. L., et al. 1997, in *Transparent Universe*, ed. C. Winkler, T. J.-L. Courvoisier, & Ph. Dourouchoux (Noordwijk ESA), 249
- Singh, N. S., Naik, S., Paul, B., et al. 2002, *A&A*, 392, 161
- Ubertini, P., Lebrun, F., Di Cocco, G., et al. 2003, *A&A*, 411, L131
- van der Klis, M., & Bonnet-Bidaud, J.-M. 1989, *A&A*, 214, 203
- van Kerkwijk, M. H., Charles, P. A., Geballe, T. R., et al. 1992, *Nature*, 355, 703
- Vedrenne, G., Roques, J.-P., Schönfelder, V., et al. 2003, *A&A*, 411, L63
- Vilhu, O., Hjalmarsdotter, L., Zdziarski, A. A., et al. 2003, *A&A*, 411, L405
- White, N. E., Nagase, F., & Parmar, A. N. 1995, in *X-ray binaries*, ed. W. H. G. Lewin et al. (Cambridge: Cambridge University press)
- Winkler, C., Courvoisier, T. J.-L., Di Cocco, G., et al. 2003, *A&A*, 411, L1